OPEN ACCESS

ACTA METALLURGICA SLOVACA

2025, VOL. 31, NO. 1, 47-52

RESEARCH PAPER

Effect of thermal exposure on the compressive strength and microstructure of Al 6061 alloy

Ketan Verma[1], Priyanshu Singh, Ayan Khan, Saurabh Dewangan[*]

Department of Mechanical Engineering, Manipal University Jaipur, Jaipur, Rajasthan, India, Pin-303007

*Corresponding author: saurabh.dewangan@jaipur.manipal.edu, tel.: 0141-3999100-838, Department of Mechanical Engineering, Manipal University Jaipur, Jaipur, Rajasthan, India, Pin-303007

Received: 13.01.2025
Accepted: 15.02.2025

ABSTRACT

Al 6061 is a commercial-grade aluminium alloy highly utilized in aerospace, automotive, high-pressure gas cylinders, and many other construction purposes. Al 6061 is a heat-treatable grade. Heat treatment can enhance the alloy's mechanical and microstructural qualities by controlling grain size and precipitate distribution. Three heat treatment steps are followed for any non-ferrous alloy to achieve the desired mechanical properties. In this work, only two heat treatment steps have been followed- solution annealing followed by quenching in three different media, i.e., water, oil, and air. The heat-treated samples' compression, hardness and microstructural properties were assessed and compared with those of untreated samples. A significant drop in the yield stress was noticed in the solutionized+quenched samples due to dissolved secondary and ternary phases in the primary α matrix. However, the improved precipitation of the secondary (Mg2Si) phase has greatly increased the hardness of the quenched sample. Optical microscopic images have observed high fine ternary Al-Mg-Si and secondary Mg2Si precipitated.

Keywords: Al 6061; Compression test; Hardness; Microscopy; EDS; XRD

INTRODUCTION

Common metals like Al, Cu, and Mg and high-strength, high-temperature alloys like W, Ta, Ti, Mo, and so on are all considered nonferrous metals and alloys. Despite often being more costly than ferrous metal, nonferrous metals and alloys have many significant uses due to characteristics including a relatively simple & economic production, low density, high thermal conductivity, and corrosion resistance [1]. Aluminum in its pure form is ductile and soft. More strength is needed for most commercial applications than pure aluminum can provide. Aluminum is a structurally lightweight material that may be reinforced by alloying and, depending on its composition, by cold working and heat treatment. To create different strength level alloys, extra elements are added to aluminum. Because aluminum and its alloys offer significant benefits, they seem to have more uses and to be competitive with ferrous alloys [2]. Si and Mg are the primary alloying elements in Al 6061, which belongs to the 6XXX series. Cu and Mn are added to improve mechanical qualities. Precipitation hardening is the physical method that works best for heat treating 6XXX alloys, and it consists of three steps: (1) Solution heat treatment- a solid solution is formed by alloying elements in this step by heating the sample to a temperature level of 350-450ºC for a period of 1-3 hr; (2) Quenching- this step is required for stabilizing the solid solution at room temperature; (3) Aging for 2 - 5 hours at temperatures between 100 and 300°C causes precipitates to develop in the fine dispersion inside the supersaturated areas [3, 4]. Medium-strength, heat-treatable Al-Mg-Si alloys (6XXX series) often resist stress corrosion cracking (SCC). The ageing precipitate Mg_2Si is the main factor that strengthens them. Magnesium and silicon are stoichiometrically balanced in Al 6061, the most widely used alloy, to create Mg_2Si. Other alloys are strengthened by adding extra Si; however, if heat treatments are not done correctly, the excess silicon alloys may become more vulnerable to stress corrosion cracking (SCC) [2].

Although heat treatment on aluminium alloys has been studied extensively, research is still ongoing. Researchers have used various methods for heating, cooling, and aging. Some of the recent works on heat treatment and mechanical property analysis on aluminum alloys are discussed here: A study examined the mechanical, fatigue, and microstructure properties of Al 6086, a novel high-strength aluminum alloy derived from Al 6082. The alloy undergoes homogenization, extrusion, and T6 heat treatment, resulting in a higher Si, Cu, and Zr content. While the alloy's ductility remains constant, its quasi-static strength is significantly greater than other Al 6XXX alloys. Fatigue tests show good resistance and are the foundation for engineering design applications [5]. The cladding quenching was used to investigate how quenching residual stress influences the precipitation behavior of slabs of Al 7085 alloy. The results showed that residual stress diminishes as the thickness of the cladding layer grows; residual stress is practically eliminated at 1-1.4 mm. This work also investigates the mechanics underlying the impact of quenching residual stress on the precipitation of the alloy Al 7085 [6]. Heat treatments' effects on the intrinsic anisotropy of Al 7075 deposits made by cold spray additive manufacturing (CSAM) are examined in a work. The findings indicate that secondary phases develop and nucleate preferentially at feeding powder particle-particle contacts. Recovery and recrystallization take place following heat treatments, however microstructural anisotropy persists. Heat treatment can reduce mechanical anisotropy, but it cannot totally eradicate it. Microhardness and ultimate tensile strength (UTS) were highest in the T6 sample. Elongation was greatly enhanced by the sintering process [7]. A study looked at how heat treatment affects the mechanical characteristics and microstructure of TiB_2/Al 2024 composites made via laser-powder directed energy deposition. The inclusion of TiB_2 results in reduced plasticity and grain refinement, according to the results. The composite material's UTS and elongation improve after 10 hours of solution treatment, whereas yield strength and microhardness reach at the peak after 15 hours [8]. The effect of excess vacancies in Al-Mg-Si alloys throughout natural and artificial ageing was studied in a work. Excess vacancies are eliminated in the first seconds of artificial aging, and equilibrium vacancies predominantly drive subsequent hardness. The data indicates that the involvement of excess vacancies in Al-Mg-Si alloys may be a universal phenomenon [9]. Aluminum alloys that have been quenched lose surplus vacancies to sinks due to gradual cooling. The natural ageing process in Al-Mg-Si alloys balances free vacancy fractions [10]. A study investigates the effects of aging treatment and quenching rate on the microstructure and characteristics of Al-Zn-Mg alloys. After being quenched in water and air, the alloy was aged for 0–120 hours at 120°C. The findings indicate that over-aging treatment impacts precipitates and precipitation-free zones less than quenching rate. Grain boundary PFZs are widened by over-aging, which damages air-quenched alloys while enhancing corrosion resistance in water-quenched alloys. Tensile and hardness characteristics are not significantly impacted by prolonged over-aging [11]. An investigation was done into the effects of thermal deformation on the microstructure and precipitation behavior of Al-Zn-Mg-Cu based Al 7055 alloy. The solution heat treated sample revealed equiaxed grains which further gets recrystallized after hot rolling [12]. This study investigates the strengthening of Al 7005 by extreme plastic deformation and ageing treatments, with a focus on pre-deformation artificial ageing and post-deformation natural ageing. The results demonstrate outstanding strengthening with a yield strength of above 400 MPa, mostly due to grain refinement, increased dislocation density, and increased precipitate volume percentage. The study found that the volume proportion of precipitates that occur during natural aging boosts strength [13]. The Al 7A99 alloy underwent various aging processes, refined coarse Mg(Zn,Cu) phases, and increased corrosion resistance through solid solution, GPI zones, metastable η′, and stable η stages [14]. A study examines the mechanical properties and microstructure development of the as-cast AZ31-1Y alloy at different cooling rates. The best mechanical properties are achieved at 29.9°C/s of cooling rate [15]. The mechanical properties of vehicle flange components of Al 6082 alloy have been analyzed after T6 heat treatment. Results show increased yield strength, ultimate tensile strength, and good elongation with optimal T6 heat treatment parameters. Tiny precipitates, β-Mg_2Si and Al(FeMn)Si, improve mechanical properties [16]. A research work looks into how solution heat treatments affect an Al–3.39%Cu–2.26%Mg alloy's microstructure, thermal, mechanical, and corrosion characteristics. Gravity dies casting was used to create the alloy from Al 5754 and Al–Cu alloys. The alloy has a brinell hardness of 77.2 HB and exhibits precipitate phases in its microstructure. Heat treatment and ageing cause the Brinell hardness to drop to 63.6 HB. Precipitate phase dissolution enhances corrosion resistance. Heat treatment raises the alloy's ultimate compressive stress [17]. A work shows how to use wire-arc directed energy deposition (DED) to produce high-performance Al-6Mg-0.3Sc alloy components without heat treatment. This results in improved mechanical properties attributed to solid solution and reinforcing grain boundaries, as well as increased yield strength, tensile strength, and elongation [18]. The cast Al-Si-10Mg alloy's microstructure, hardness, tensile strength, and dry wear characteristics were investigated in a study. The alloy underwent air cooling, quenching, and T6 treatment after being created using gravity die casting. The T6 treatment changed the microstructure to a spherical shape, resulting in β-Mg_2Si precipitates and Si particle spheroidization. Wear resistance, tensile strength, and yield strength rose by 70% after following aging process [19]. The mechanical characteristics and microstructure development of Al 6082 alloy were analyzed after processing through deep cryogenic-aging treatment (DCAT), artificial aging treatment (AAT), and solid solution treatment (SST). According to the results, SST specimens exhibited the highest elongation, in-plane anisotropy, and lowest yield strengths. AAT specimens decreased maximum elongation and IPA while increasing yield strengths. The strongest dislocation pinning effect was seen in DCAT alloys, which led to increased yield strength [20]. A work examined the microstructure of an Al-Si-Mg alloy after adding Mn and heating. Results showed a Mn-rich $Al_{15}Mn_3Si_2$ phase and a Mg-rich $Al_5Si_3Mg_2$ phase. Heat treatment increased hardness and tensile strength and enhanced electrical resistance [21]. With an emphasis on the η-phase precipitates that nucleate heterogeneously on grain boundaries and are associated with the quench sensitivity of aluminum alloys in the 7xxx family, the study investigates the effects of cooling rates on the composition of quench-induced grain boundary precipitates [22]. The effect of aging on the mechanical characteristics of the Al18Si3.6Cu0.34Ce alloy was assessed. After undergoing T6 heat treatment for varied lengths of time, the alloy's shape and spheroidization changed. The findings demonstrated that aging increased the as-cast alloy's yield strength and ultimate tensile strength. Additionally, flow stress improved with aging, mostly because of homogeneity. Along with enhanced load bearing and shear strength capacity, the aging process has increased the wear resistance of the alloy [23]. The effect of addition of magnesium on the microstructure and mechanical characteristics of Al-Cu-Mg alloys was analyzed. Because of high strength-to-weight ratio, cast Al-Cu-Mg alloys are employed in various applications. According to the study, adding 0.5 to 2.5% magnesium enhanced hardness by 22% and tensile strength by 69.9%. Grain refinement and mechanical qualities were also impacted by aging, with 1% Mg having a major impact because of the reduced grain size [24]. Pre-aging and thermomechanical treatment were combined to improve the hardness and corrosion resistance of the Al 7075 alloy. Transmission electron microscopy was used to view the alloy's microstructure and investigate the connection between changes in performance and microstructure evolution. More matrix precipitates boosted the alloy's hardness, and rounder grain boundary precipitates improved its resistance to corrosion [25]. The effect of thermal treatment parameters and microalloying components on the mechanical and thermal characteristics of modified Al-Zn-Mg-Cu-X alloy has been assessed in a work. Although T6 aging increases tensile strength by 30%, adding 0.25 weight% of scandium (Sc) refines grain structure, raises precipitate percentage, and reduces grain size [26]. The microstructural variation at the welded joint of Al 6061 alloy has been analysed, and its effect on the strength has been checked. The water quenching phenomenon was highly beneficial for increasing the tensile strength of the welded joint [27, 28].

In previous studies, the researchers have used three steps of heat treatment, which include solution annealing, quenching and then aging. The last step of aging involves a prolonged heating of aluminium alloy in which the supersaturated solid solution transforms into precipitate particles that can greatly enhance the strength of the alloy. Although aging improves the strength of the alloy, it takes a high energy consumption for a long duration. In this direction of research, the present work focuses on two steps of heat treatment on Al 6061 alloy. These two steps include solution annealing and then quenching. Three quenching media, such as, water, oil, and air were used in this work because they provided three different cooling rates to the Al 6061 alloy. Based on that, heat-treated samples' compressive strength and hardness characteristics were analyzed. A corroboration between microstructure and mechanical properties has been established.

MATERIALS AND METHODOLOGY

The Al 6061 alloy was taken in the form of cylinders with length and diameter of 70 mm and 35 mm, respectively. To verify the constituent elements of this alloy, EDS analysis was carried out. **Fig. 1** shows the EDS spectra along with the Wt% and atomic% of each constituent element.

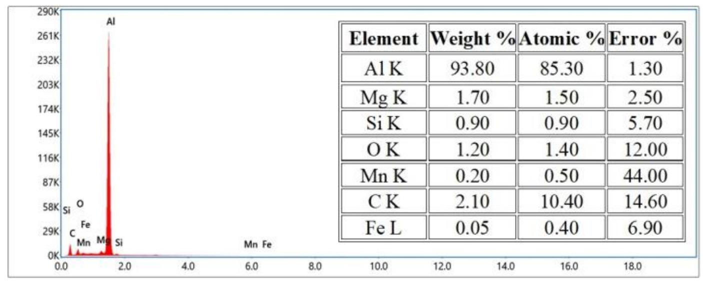

Element	Weight %	Atomic %	Error %
Al K	93.80	85.30	1.30
Mg K	1.70	1.50	2.50
Si K	0.90	0.90	5.70
O K	1.20	1.40	12.00
Mn K	0.20	0.50	44.00
C K	2.10	10.40	14.60
Fe L	0.05	0.40	6.90

Fig. 1 EDS spectroscopy of Al alloy under study showing various elements of the metal

Also, XRD analysis was carried out to check the availability of various phases and compounds at the 2θ range of 30°-90° (**Fig. 2**). The high intensity peaks of Al were recorded on the planes of 111, 002, 022, 113, and 222 at 2θ of 39°, 44°, 66.5°, and 78.4° respectively. Other than these, small peaks of Mg_2Si compound were also recorded at 2θ of 35° and 42°. The XRD results were matched and referred to [29-31].

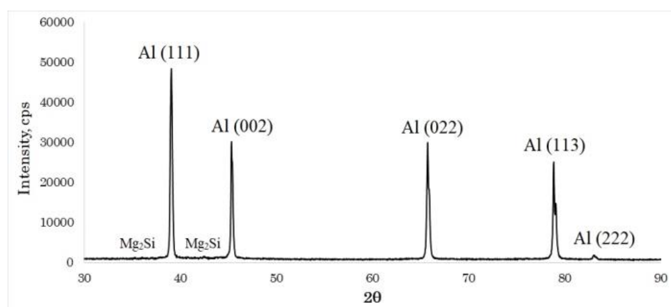

Fig. 2 XRD result of Al 6061 alloy considered in the work

A total of four such cylinders were taken in this study. The samples' shape and size were considered cylindrical rods for compression tests. The sample-1 was kept in standard condition. Samples 2, 3 and 4 were heated in the furnace at 400ºC for 4 hr. Sample 2 was taken from the furnace for cooling purposes and quenched into water. Sample 3 was dipped into mustered oil, and sample 4 was left in the atmosphere for cooling till room temperature. A room temperature of 30 °C was considered to determine the cooling rate in each case. The cooling rates in samples 2, 3 and 4 were 12.33°C/s, 0.2°C/s, and 0.05°C/s, respectively. In this work, only two steps have been taken, i.e., solution treatment and quenching. The third step of 'aging' has not been performed.

An optical microscopic examination was performed to analyse the microstructural characteristics of each plate after the heat treatment. Two magnifications of 200X and 500X were used to obtain various structures to get the microscopic photos. The samples were polished using five different grades of abrasive papers with grit sizes 500, 1000, 1600, 2500, and 3200. Upon polishing, the surface of every sample was etchant-treated using Keller's reagent.

Upon heat treatment, all the samples were tested on universal testing machine (UTM-400kN capacity) for their compressive nature. To make proper comparison among them, a common maximum load of 202 kN (± 3kN) was applied on all the four samples and the deformation was recorded during the compression. The load was applied at a common speed of 5 mm/min on every specimen. The samples before and after the compression test are shown in **Fig. 3 (a, b)**. The hardness was tested on all the samples by macro-Rockwell hardness tester machine with a load of 100 kgf. For measuring hardness in the samples, 1/16th ball indenter was used in Rockwell hardness tester, resulting in hardness values in B-scale (HRB). Four indents were made in each sample, and an average hardness was found for that sample.

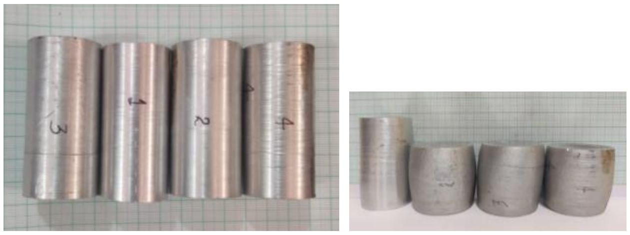

(a) (b)

Fig. 3 (a) Four cylindrical shaped samples used for compression test; (b) The samples after compression test: from left to right- sample-1, 2, 3 and 4.

RESULT ANALYSIS AND DISCUSSION

The compression test analysis: The compression test results were obtained as load-displacement curves for each sample. As shown in **Fig. 3**, the least deformation was obtained in sample 1, which was not heat-treated. Remaining three samples have got deformed till a certain height after the heat treatment. The maximum displacement recorded in sample was 11.3 mm. This sample has shown a yield strength of 194 MPa. Sample 2 has been water quenched. After a load exertion of 203.7 kN, it has been deformed till 26.3 mm. This displacement is nearly 133% higher than in sample 1. Also, the yield point has been attained quite earlier than the same of sample 1. The yield strength of sample 2 is 65 MPa. Sample 3, an oil quenched sample has shown a similar attributes of compression test results as sample 2. The maximum displacement of 25.8 mm was recorded after a maximum load application of 203 kN. The yield strength reported in sample 3 was 67 MPa. The displacement and yield strength of sample 3 are nearly 128% higher and 65% lower, respectively, than sample 1. Sample 4, being air cooled, has shown the maximum elongation of 27 mm with a compressive load of 201 kN. Also, the yield stress in sample 4 is the lowest among all. In comparison to sample 1, the air-cooled sample possessed nearly 141% higher elongation and 69% lower yield stress. It means, a faster cooling process can be more beneficial to retain yield stress than lower cooling process. It is so because the quenching process produces supersaturated solid solution with constituent alloying elements. According to [32], Even if the quenching process produces a supersaturated solid solution, the solution treatment dissolves the precipitates. As a result, the heat treatment removes the strengthening effect, decreasing yield stress while boosting elongation. A comparative load-displacement graphs of all the samples are shown in **Fig. 4**. Also, the observations obtained by compression test are listed in **Table 1**.

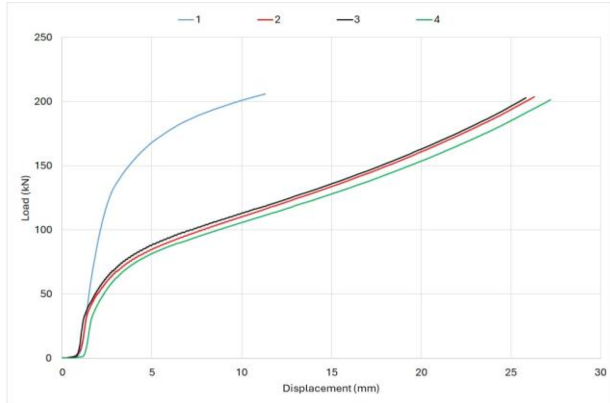

Fig. 4 Load-displacement curves obtained by compression test

Table 1 The key observation noted by compression test

Sample	Max force (kN)	Max displacement (mm)	Yield stress (MPa)
1	205.9	11.3	194
2	203.7	26.3	65
3	202.9	25.8	67
4	201.5	27.2	60

The hardness test analysis: The average hardness obtained in samples 1, 2, 3, and 4 is 18.5 HRB, 74.2 HRB, 70.5 HRB, and 72.7 HRB, respectively. An inverse relationship was seen between the yield strength and hardness in the samples. Sample 1, which has the highest yield stress, possessed a minimum hardness of 18.5 HRB. In contrast, the water-quenched sample showed a maximum hardness of 74.2 HRB.

All three heat-treated samples possess more than 280% hardness than that of sample 1 (untreated sample). Because of the quicker quenching rate, the water-quenched sample had a higher hardness than the oil and air-quenched samples. A fast-quenching phenomenon causes a high density of vacancies and increased supersaturation in the solid solution. This supersaturation promotes the production of fine and evenly dispersed ternary Al-Mg-Si precipitates, which harden the alloy's surface. **Fig. 5** shows the comparative bar chart of hardness along with the microstructure of the samples.

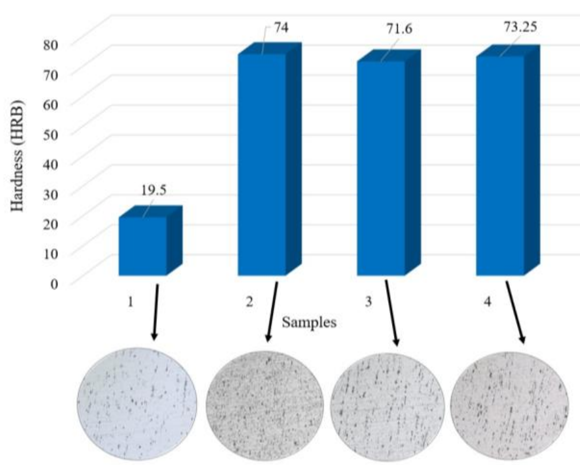

Fig. 5 Hardness and its analysis of untreated and heat-treated samples according to microstructural appearance

The microstructural analysis: The microstructural images were captured after the heat treatment and the compression test. The microstructure of the Al 6061 alloy consists of brilliant primary α-Al, dark Mg_2Si precipitates, and fine ternary phase of Al-Mg-Si (**Fig. 6a**).

(a) Sample-1

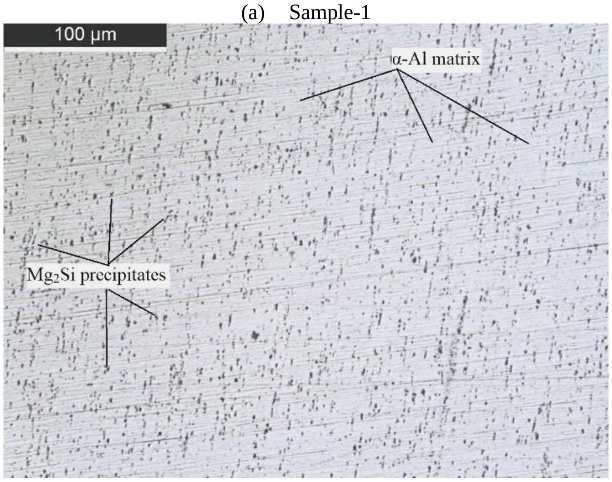

(b) Sample-2

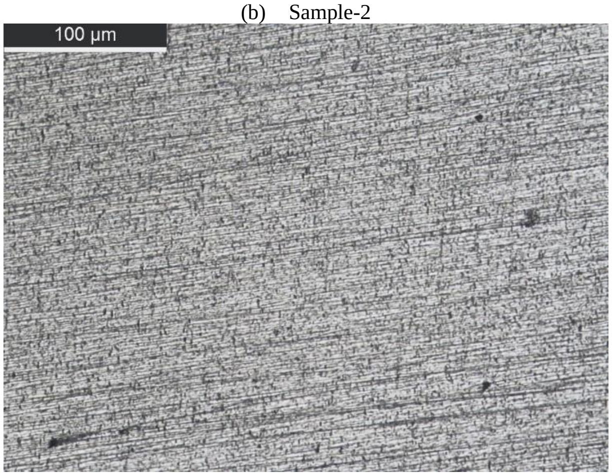

(c) Sample-3

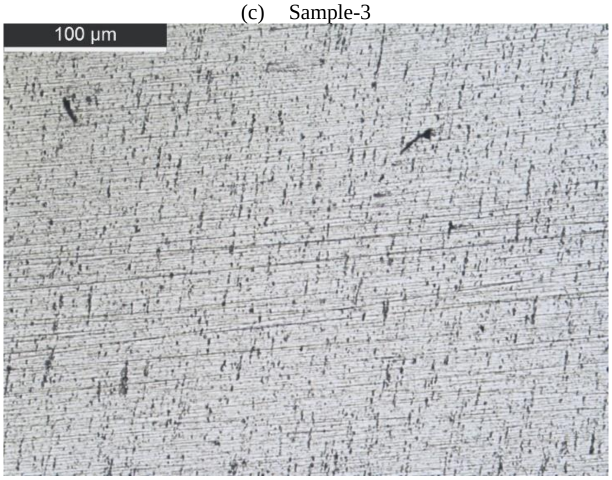

(d) Sample-4

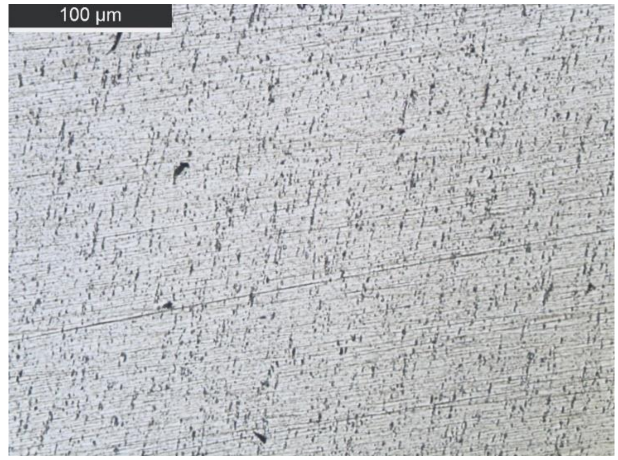

Fig. 6 Microstructure of Al 6061 alloy used under study (Magnification = 200X)

Sample 1 is cold rolled, with α grains (elongated towards the rolling direction) and bands of Mg2Si precipitates. After 400oC solution treatment, the three samples' elongated α shape becomes equiaxed, and Mg2Si precipitates are evenly distributed. According to [33-35], after solutionizing at 500°C, recrystallization phenomenon occurs. As a result, the microstructure gets converted into equiaxed and defect-free grains. The majority of Mg2Si precipitates were found along the principal α borders. **Fig. 6(b)** shows that the water quenching process has increased the precipitation of Mg2Si over the α-Al matrix. In addition, the exposure of the ternary Al–Mg–Si phase has also increased, making sample 2 hard. Similarly, the oil quenching (**Fig. 6c**) and air quenching (**Fig. 6d**) processes have vouched for the precipitation of the Mg_2Si secondary phase.

Fig. 7 shows the microstructural images at 500X magnification in which the ternary Al-Mg-Si fine precipitates can be observed clearly. Compared to sample 1, all the heat-treated samples have significantly improved the secondary and ternary phases over the Al-matrix. In addition, the α-boundary thickness gets increased after solution heat treatment. It happened due to displacement of ternary Al–Mg–Si phase towards primary-Al grain boundary. The heat-treated samples have shown higher elongation and lower yield stress than untreated sample 1.

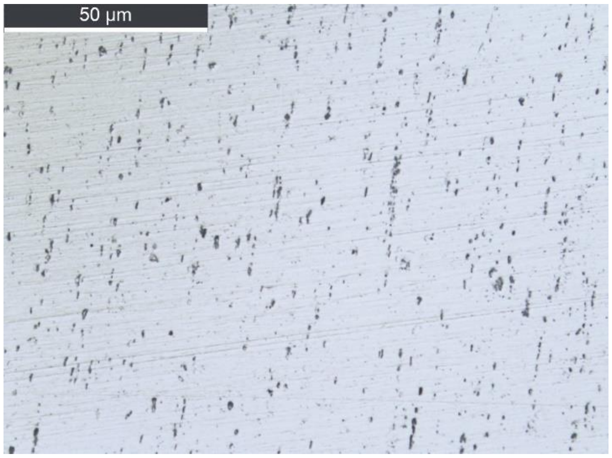

(a) Sample-2

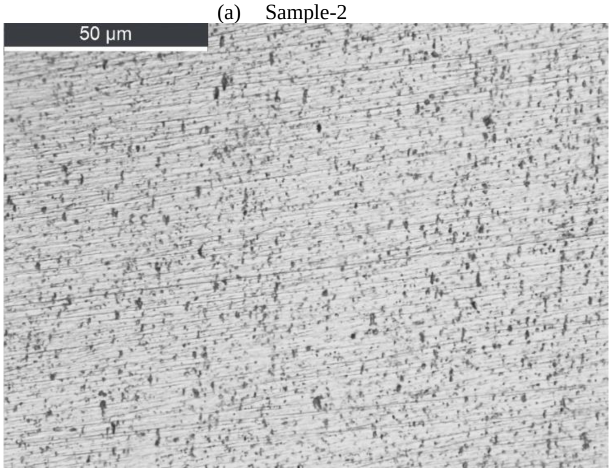

(b) Sample-3

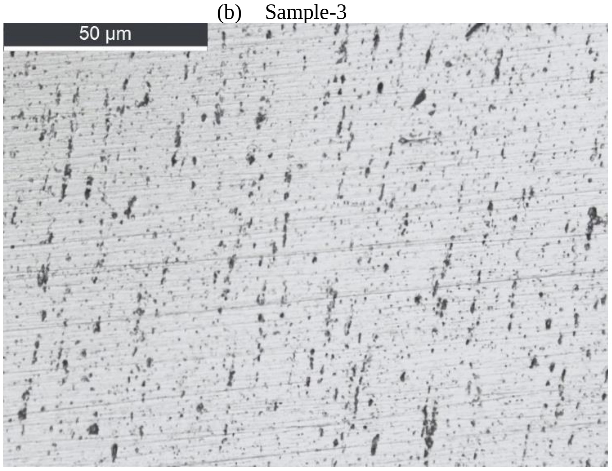

(c) Sample-4

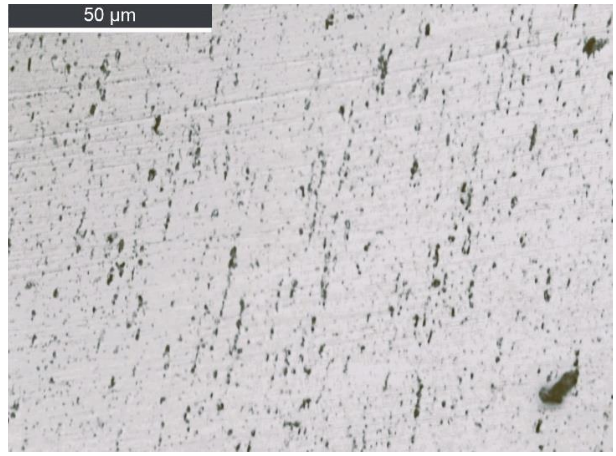

Fig. 7 Microstructure of Al 6061 at magnification of 500X

CONCLUSION

The following conclusions can be drawn from this work:

1. According to EDS and XRD data, Mg and Si are few in Al 6061 alloy, yet they affect the alloy's mechanical characteristics.
2. The microstructural analysis revealed the elongated primary α-Al, secondary Mg_2Si precipitates, and fine Al-Mg-Si ternary eutectic in the untreated cold-rolled sample 1. The solution treatment leads to recrystallisation, and the elongated α becomes an equiaxed shape. After quenching, the secondary and ternary phases are dissolved into the α matrix.
3. Because of the strong secondary (Mg_2Si) phase precipitation, the water-quenched sample had the highest hardness among all heat-treated samples.
4. When the solution is quenched, the fine ternary phases are shifted towards the primary α border, causing the samples to deform easily during compression loading. Thus, after employing three quenching techniques, the yield stress was reduced by about 65%.

In the present work, only two steps of heat treatment, solution annealing and quenching, have been adopted to save energy involved in prolonged heating during the aging process. In future work, three steps of heat treatment will be carried out on the same grade of aluminium alloy, and the mechanical properties will be compared with the results of the present study.

REFERENCES

[1] S. Kalpakjian, S. R. Schmid: Manufacturing engineering and technology, Saddle River, New Jersey: Prentice Hall, 2010.
[2] J.E. Hatch: *Aluminum Properties and Physical Metallurgy*. Chapter 5, Ohio: ASM International, 1, 1984, 134-199.
[3] W.D. Callister Jr, D.G. Rethwisch: *Callister's materials science and engineering*, Hoboken, New Jersey: John Wiley & Sons, 2020.
[4] G. Mrówka-Nowotnik, J. Sieniawski: Journal of Materials Processing Technology, 162, 2005, 367-372. https://doi.org/10.1016/j.jmatprotec.2005.02.115
[5] F. Zupanič, J. Klemenc, M. Steinacher, S. Glodež: Journal of Alloys and Compounds, 941, 2023, 168976. https://doi.org/10.1016/j.jallcom.2023.168976
[6] J. Liu, Z. Du, J. Su, J. Tang, F. Jiang, D. Fu, J. Teng, H. Zhang: Journal of Materials Science & Technology, 132, 2023, 154-165. https://doi.org/10.1016/j.jmst.2022.06.010
[7] Y. Ren, D. Zhou, G. Xie, H. Liu, X. Cui, J. Wang, T. Xiong: Materials Characterization, 199, 2023, 112828. https://doi.org/10.1016/j.matchar.2023.112828
[8] B. Chen, X. Xi, T. Gu, C. Tan, X. Song: Journal of Materials Research and Technology, 9(6), 2020, 14223-14236. https://doi.org/10.1016/j.jmrt.2020.10.014
[9] Z. Yang, J. Banhart: Acta Materialia, 215, 2021, 117014. https://doi.org/10.1016/j.actamat.2021.117014

[10] Z. Yang, X. Jiang, X. Zhang, M. Liu, Z. Liang, D. Leyvraz, J. Banhart: Scripta Materialia, 190, 2021, 179-182. https://doi.org/10.1016/j.scriptamat.2020.08.046
[11] F. Jiang, J. Huang, Y. Jiang, C. Xu: Journal of Alloys and Compounds, 854, 2021, 157272. https://doi.org/10.1016/j.jallcom.2020.157272
[12] M. Zhang, C. Li, Y. Zhang, S. Liu, J. Jiang, J. Tang, L. Ye, X. Zhang: Materials Characterization, 172, 2021, 110861. https://doi.org/10.1016/j.matchar.2020.110861
[13] R. Bakhshi, M.H. Farshidi, S.A. Sajjadi: Transactions of Nonferrous Metals Society of China, 31(10), 2021, 2909-2921. https://doi.org/10.1016/S1003-6326(21)65702-3
[14] Y. Hou, L. Chen, Z. Li, G. Zhao, C. Zhang: Materials Science and Engineering: A, 780, 2020, 139217. https://doi.org/10.1016/j.msea.2020.139217
[15] L. Zai, X. Tong, H. Zhang, X. Xue: Journal of Materials Research and Technology, 28, 2024, 3449-3462. https://doi.org/10.1016/j.jmrt.2023.12.267
[16] J. Jiang, J. Cui, Y. Wang, M. Huang, J. Dong, J. Yan: Materials Science and Engineering: A, 912, 2024, 146974. https://doi.org/10.1016/j.msea.2024.146974
[17] N. Patel, M. Joshi, A. Singh, G.N. Mittal, M. Agrawal, S. Manani, A.K. Pradhan: International Journal of Metalcasting, 18(2), 2024, 1151-1159. https://doi.org/10.1007/s40962-023-01095-6
[18] K. Li, X. Fang, J. Yang, X. Li, M. Ma, J. Shang, K. Huang: Journal of Manufacturing Processes, 125, 2024, 589-603. https://doi.org/10.1016/j.jmapro.2024.07.088
[19] M. Beder, S.B. Akçay, T. Varol, H. Çuvalcı: Arabian Journal for Science and Engineering, 2024, 1-12. https://doi.org/10.1007/s13369-024-08971-1
[20] E. Xia, T. Ye, S. Qiu, J. Liu, J. Luo, L. Sun, Y. Wu: Coatings, 14(5), 2024, 602. https://doi.org/10.3390/coatings14050602
[21] Y. Kaygısız, Ç. Palta, T.Ç. Kaymaz, S. Engin: International Journal of Metalcasting, 18(3), 2024, 2283-2297. https://doi.org/10.1007/s40962-023-01165-9
[22] Y. Yao, R. Euesden, M.E. Curd, C. Liu, A. Garner, T.L. Burnett, P. Shanthraj, P.B. Prangnell: Acta Materialia, 262, 2024, 119443. https://doi.org/10.1016/j.actamat.2023.119443
[23] K. Gangal, K. Devendra: Advances in Materials and Processing Technologies, 10(3), 2024, 2122-2144. https://doi.org/10.1080/2374068X.2023.2206198
[24] S.A. Salihu, A. Isah, P. Evarastics: IOSR Journal of Pharmacy and Biological Science, 4, 2012, 15-20.
[25] W. Zhang, R. Su, G. Li, Y. Qu: Journal of Alloys and Compounds, 960, 2023, 170953. https://doi.org/10.1016/j.jallcom.2023.170953
[26] D. Mukherjee, H. Roy, B. Chandrakanth, N. Mandal, S.K. Samanta, M. Mukherjee: Materials Chemistry and Physics, 314, 2024, 128881. https://doi.org/10.1016/j.matchemphys.2024.128881
[27] A. Ayush, S. Dewangan, S. Ishwar, A. Agarwal: World Journal of Engineering, 2024. https://doi.org/10.1108/WJE-05-2024-0309
[28] A.P. Reddy, S. Dewangan: Acta Metallurgica Slovaca, 29(2), 2023, 75-81. https://doi.org/10.36547/ams.29.2.1778
[29] K. Thirumavalavan, L. Karunamoorthy, K.A. Padmanabhan: International Journal of Engineering and Technology, 6, 2014, 1026-1032.
[30] Z. Nikseresht, F. Karimzadeh, M.A. Golozar, M. Heidarbeigy: Materials & Design, 31(5), 2010, 2643-2648. https://doi.org/10.1016/j.matdes.2009.12.001
[31] C. Zeng, H. Ghadimi, H. Ding, S. Nemati, A. Garbie, J. Raush, S. Guo: Materials, 15(10), 2022, 3676. https://doi.org/10.3390/ma15103676
[32] M. Carta, L. Aydi, P. Buonadonna, D. Morea, M. El Mehtedi: Heliyon, 10(23), 2024. https://doi.org/10.1016/j.heliyon.2024.e40922
[33] K. Liu, C. Li, X.G. Chen: MATEC Web of Conferences, 326, 2020, 03001). https://doi.org/10.1051/matecconf/202032603001
[34] C. Pillajo et al.: Canadian Metallurgical Quarterly, 60*(4)*, 2021, 359-365. https://doi.org/10.1080/00084433.2021.2014724
[35] Y. Pazhuhanfar, B. Eghbali: International Journal of Minerals, Metallurgy and Materials, 28(6), 2021, 1080-1089. https://doi.org/10.1007/s12613-021-2288-0